

CEBAF PROPOSAL COVER SHEET

This Proposal must be mailed to:

CEBAF
Scientific Director's Office
12000 Jefferson Avenue
Newport News, VA 23606

and received on or before OCTOBER 30, 1989

TITLE:

Measuring the Number of Pions in the Nucleus

CONTACT
PERSON:

C. C. Chang

ADDRESS, PHONE
AND BITNET:

Dept. of Physics, University of Maryland
(301) 454-5779
CHANG@UMDENP

THIS PROPOSAL IS BASED ON A PREVIOUSLY SUBMITTED LETTER
OF INTENT

☒ YES
☐ NO

IF YES, TITLE OF PREVIOUSLY SUBMITTED LETTER OF INTENT

Measuring the Number of Pions in the Nucleus

ATTACH A SEPARATE PAGE LISTING ALL COLLABORATION
MEMBERS AND THEIR INSTITUTIONS

=====

(CEBAF USE ONLY)

Letter Received 10-31-89

Log Number Assigned PR-89-035

by KES

contact: Chang

RESEARCH PROPOSAL TO CEBAF

30 October 1989

MEASURING THE NUMBER OF PIONS IN THE NUCLEUS

THE HALL A COLLABORATION

American University, Cal. State University LA,
Case Western Reserve and LANL, CEBAF, George Washington University,
University of Georgia, Indiana University Cyclotron Facility,
Kent State University, University of Maryland,
Massachusetts Institute of Technology,
University of New Hampshire, National Institute of Science and Technology,
Norfolk State University, University of Regina, University of Rochester,
University of Saskatchewan, Rutgers University, Stanford University,
University of Virginia, University of Washington,
College of William and Mary, NIKHEF-K, CEN Saclay,
University of Clermont-Ferrand, INFN Sezione Sanita, University of Lund,

Spokesperson

C. C. Chang, University of Maryland
J. S. O'Connell, NIST
R. Gilman, Rutgers University

ABSTRACT

The exchange of pions by nucleons inside the nucleus creates a population of constituent pions. The spectral function of this population can be measured in an $(e, e'\pi)$ experiment using quasifree kinematics with excitation above the nucleon resonance region. A longitudinal-transverse separation at low four-momentum transfer helps distinguish pion creation on the nucleon from knockout of the constituent pions. The momentum and binding energy distributions of the pions in the nuclear ground state can be inferred from the coincidence measurement of the missing-momentum and missing-energy spectra. The pion spectral function is connected theoretically to the two-nucleon potential and the low-energy pion-nucleus optical potential.

I. INTRODUCTION

Bound nucleons exchanging pions with their neighbors create a population of virtual pions inside the nucleus. The number of pions (in excess of those associated with free nucleons) is a theoretically calculable and an experimentally measurable quantity. Recent calculations¹⁻³ of the pion density give, for medium weight nuclei, one exchange pion present at any time for every eight nucleons, and this density is nuclear mass dependent.

The nuclear medium effects on the nucleon structure have recently been demonstrated by the EMC effect⁴; i.e., the structure function of the nucleon embedded in the nucleus is different from that measured on a free nucleon. One possible explanation is that there are more pions per nucleon in the nucleus than in nucleon.

We propose to measure the number and spectral function of these constituent pions with the reaction $A(e, e'\pi)$ in quasifree kinematics detecting pions near the direction of the three-momentum transfer to the nucleus and with pion energies near the energy loss of the scattered electron. The analysis philosophy is similar to that used to extracting the bound nucleon spectral function from $(e, e'N)$ measurements. The experiment will be performed in the excitation energy region above the nucleon resonances and at low four-momentum transfer. These kinematic variables are chosen so that the contributions from the creation of pions on the nucleon and pions from the hadronizing quarks would be minimized.

The measurement would be made first on hydrogen and deuterium (as a benchmark of pions associated with free nucleons) and then on a series of targets with increasing A . A longitudinal-transverse separation will be made on the data to isolate the pion pole term which dominates the longitudinal cross section to further minimize the contribution of pion creation on the nucleon which is mainly a transverse process.

II. THEORETICAL ESTIMATES

The spectral function of the number of pions per nucleon in a nucleus is given by

$$S_{\pi}(p, E) = \langle \Psi | a_{\pi}^{\dagger} a_{\pi} | \Psi \rangle / A \quad (1)$$

where Ψ is the nuclear ground state wave function and $a_{\pi}^{\dagger}a_{\pi}$ is the number operator for a pion of momentum p and total energy E . The density due to exchange pions is obtained by subtracting the contribution of the pion cloud around a free nucleon ψ ,

$$\rho_{\pi}(p, E) = S_{\pi}(p, E) - \langle \psi | a_{\pi}^{\dagger} a_{\pi} | \psi \rangle. \quad (2)$$

The total number of these exchange (or constituent nuclear) pions is then

$$N_{\pi} = \int \rho_{\pi}(p, E) d^3p dE. \quad (3)$$

A calculation of these quantities has been made in Ref. 1 in which a Hamiltonian for the πNN and πNA interactions are used in a variation calculation for $\rho_{\pi}(p, E)$. Figure 1 shows a plot of the momentum density and Table 1 gives the numbers of constituent pions as a function of atomic weight.

In Ref. 2 similar conclusions are reached by a different calculational technique. The pion spectral function is computed from the response function $R(p, E)$ derived from the pion-nucleus optical potential

$$S_{\pi}(p, E) = \frac{1}{\pi} \frac{\text{Im } R(p, E)}{(E + E_0)^2} \quad (4)$$

where E_0 is the on-shell pion energy for momentum p . Figure 2 shows the spectral function associated with the MSU pion-nucleus optical potential.⁵

A third theoretical approach to the pion momentum distribution is pursued in Ref. 3 where the one pion exchange potential is used directly

$$\rho(p, E) = - \frac{1}{A} \langle \Psi | \frac{V_{\text{ope}}(p)}{E} | \Psi \rangle. \quad (5)$$

The conclusions are similar to those of Refs. 1 and 2. The authors of Ref. 3 then use the pion distribution function to explain the EMC effect.

We see that the proposed $(e, e' \pi)$ measurement allows us to check the connection of the constituent pion spectral function to other fundamental nuclear quantities: the πNN and πNA vertex functions, the pion-nucleus optical potentials, and the NN pion exchange potential.

III. EXPERIMENTAL APPROACH

III.1. Notation and Kinematics

We use the reaction $e+p \rightarrow e'+\pi^++n$ as an example to define the kinematics of pion electroproduction (see Fig. 3). The four vectors in the laboratory system describing the pion leptonproduction are defined as usual:

$$e = (E_e, \vec{p}_e) = \text{incident electron} \quad (6)$$

$$e' = (E'_e, \vec{p}_{e'}) = \text{scattered electron} \quad (7)$$

$$p = (m_p, \vec{0}) = \text{target proton} \quad (8)$$

$$\pi = (E_\pi, \vec{p}_\pi) = \text{produced pion} \quad (9)$$

$$n = (E_n, \vec{p}_n) = \text{final neutron (or sum of final hadrons)}. \quad (10)$$

By measuring in coincidence the scattered electron and the produced pion, it is possible to identify the final hadrons by their missing mass $M_x^2 = (e - e' + p - \pi)^2$. We will also define the following Lorentz invariants to describe the kinematics:

$$\begin{aligned} \gamma^{*2} &= (e - e')^2 = -Q^2 \\ &= \text{squared mass of the virtual photon;} \end{aligned} \quad (11)$$

$$\nu = E_e - E'_e = \text{energy loss of the electron;} \quad (12)$$

$$\begin{aligned} s &= W^2 = (\gamma^* + p)^2 \\ &= \text{squared invariant mass of the } \gamma^* \text{-N system;} \end{aligned} \quad (13)$$

$$\begin{aligned} t &= (\gamma^* - \pi)^2 \\ &= \text{squared momentum transfer onto the target nucleon.} \end{aligned} \quad (14)$$

We have

$$Q^2 = 4 E_e E'_e \sin^2(\theta_e/2) \quad (15)$$

$$s = W^2 = m_p^2 + 2m_p \nu - Q^2. \quad (16)$$

III.2. Super-Rosenbluth Separation

The cross section for the reaction $e+p \rightarrow e'+\pi+X$ can be written in the following way:

$$\begin{aligned}
\frac{d^4\sigma(q, \nu, \theta_e, p_\pi, \theta_{p_\pi q})}{d\Omega_e d\nu d\Omega_\pi dp_\pi} &= \frac{d^4\sigma_T(q, \nu, \theta_e, p_\pi, \theta_{p_\pi q})}{d\Omega_e d\nu d\Omega_\pi dp_\pi} + \\
&\epsilon \cdot \frac{d^4\sigma_L(q, \nu, \theta_e, p_\pi, \theta_{p_\pi q})}{d\Omega_e d\nu d\Omega_\pi dp_\pi} + \epsilon \cdot \cos 2\phi \cdot \frac{d^4\sigma_P(q, \nu, \theta_e, p_\pi, \theta_{p_\pi q})}{d\Omega_e d\nu d\Omega_\pi dp_\pi} + \\
&\sqrt{2\epsilon(\epsilon+1)} \cdot \cos \phi \cdot \frac{d^4\sigma_I(q, \nu, \theta_e, p_\pi, \theta_{p_\pi q})}{d\Omega_e d\nu d\Omega_\pi dp_\pi}
\end{aligned} \tag{17}$$

where $q = |\vec{p}_e - \vec{p}_e'|$, ϕ is the angle between the pion production plane and the electron scattering plane (see Fig. 3), and ϵ is the polarization parameter of the virtual photon, and is given by:

$$\epsilon = \left(1 + 2 \frac{Q^2 + \nu^2}{Q^2} \tan^2(\theta_e/2) \right)^{-1}. \tag{18}$$

The cross sections σ_T , σ_L , σ_P and σ_I are due to the interaction of virtual photons of the following types:

- σ_T : unpolarized transverse photons;
- σ_L : longitudinal polarized photons;
- σ_P : transverse linearly polarized photons;
- σ_I : interference of transverse and longitudinal polarized photons

σ_P and σ_I can be determined through the ϕ dependence of the cross section. With the finite angular acceptance of the spectrometers in Hall A, these separations can be done in some kinematic regions. But in order to separate σ_L and σ_T it is necessary to measure the cross section for different values of ϵ with the same kinematic invariants Q^2 , s , and t (see Table 2).

The separation of the longitudinal cross section is necessary because the knockout of constituent pions occurs mainly through the coupling of the virtual photon to the charge of the pions (the pole term) which is a longitudinal process. Pion production from the nucleon is mainly a transverse process.

The longitudinal cross section for pion knockout in the quasifree approximation is given by

$$\frac{d^4\sigma_L(q, \nu, \theta_e, p_\pi, \theta_{p_\pi q})}{d\Omega_e d\nu d\Omega_\pi dp_\pi} = \sigma_m p_\pi E_\pi f_\pi^2(Q^2) S_\pi(p, E) \quad (19)$$

where σ_m is the Mott cross section, p_π and E_π are the momentum and total energy of the detected pion, and $f_\pi(Q^2)$ is the form factor of the pion. In this approximation the initial momentum p and energy E of the pion are given by the missing momentum and missing energy

$$p_m = |\vec{q} - \vec{p}_\pi|, \quad E_m = \nu - E_\pi. \quad (20)$$

Thus a measurement of $d^4\sigma_L$ is easily translated to $S_\pi(p, E)$ in the quasifree approximation.

Theoretical corrections to this simple scheme will have to be made to account for pion-nucleus interaction in the final state. Glauber multiple scattering theory is reliable for pions above 2 GeV/c in nuclei.

III.3. Choice of Kinematics

We will make the following kinematic choices:

(1) Choose an electron energy loss above the nucleon resonance region to minimize the number of pions created on nucleons by the virtual photon:

$$\nu \geq 2.0 \text{ GeV}. \quad (21)$$

(2) Choose a low value of the four-momentum transfer to avoid suppression of the cross section due to the pion form factor. However, due to the limitation on the smallest angle that the spectrometer in Hall A can have under the current design plan ($\theta_{\min} = 12.5^\circ$), we have chosen

$$Q^2 = 0.55 \text{ (GeV/c)}^2. \quad (22)$$

With these kinematic constraints, the two kinematic settings for making a Rosenbluth separation of the longitudinal cross section from other components of the cross section, assuming a maximum incident electron energy of 4 GeV, are listed in Table 2.

It is obvious from Eqs. (2) and (3) that two-dimensional spectral func-

tion over a wide range of pion momentum p and energy E is needed. An estimate of these ranges can be made based on the theoretical predictions, as shown in Figs. 1 and 2. They are:

$$\text{range of } p: 0 - 1 \text{ GeV}/c \quad (23)$$

$$\text{range of } E: 0 - 0.3 \text{ GeV}. \quad (24)$$

For a given electron kinematics, p and E (which are equal to the missing momentum and missing energy as defined in Eq. (20)) can be varied by changing the observed pion momentum $|\vec{p}_\pi|$ and its detection angle with respect to the direction of the three-momentum transfer \vec{q} . As can be seen from Fig. 4, E_m changes more rapidly by changing p_π while keeping $\theta_{p_\pi q}$ (the angle between \vec{p}_π and \vec{q}) fixed. On the other hand, p_m changes more rapidly by varying $\theta_{p_\pi q}$ while keeping $|\vec{p}_\pi|$ fixed. To cover the ranges of p and E as given by Eqs. (23) and (24), cross section measurement would have to be made over a variable range of

$$\text{pion angular range } \theta_{p_\pi q} \approx 25^\circ \quad (25)$$

$$\text{pion momentum range: } 15\%. \quad (26)$$

IV. EXPERIMENTAL SETUP

We propose to use the dual spectrometers in Hall A to detect the scattered electrons and coincident charged pions. Three liquid cryogenic targets (H_2 , D_2 , and 4He) will be required together with a number of solid targets that span the periodic table (e.g., C, Al, Fe, Ag, and W). The only special requirement of this measurement is the need for good particle identification in both the electron and hadron spectrometers. Table 3, to be discussed in the next section, shows that large numbers of unwanted particles will be found in each spectrometer at the two kinematic settings. Both spectrometers will need a gas Cerenkov detector and a shower counter (at least for the electron arm) in addition to the time-of-flight information in order to identify particles.

The angular acceptances of both spectrometers in Hall A are $\pm 1.72^\circ$ horizontally and $\pm 3.72^\circ$ vertically. To cover the pion angular range of about 25° and the momentum range of about 15% (see Eqs. (25) and (26)), we need approximately eight settings of the pion angle and two settings of the

magnetic field at each angle of the hadron spectrometer in order to sample the two-dimensional pion spectral function.

V. COUNTING RATE ESTIMATES

Tables 2 and 3 show single-arm and coincident cross sections estimated from models of nuclear reaction at high excitation energy⁶ and from measured $H(e, e' \pi^+)$ cross section.⁷ The counting rates are then calculated based on the following Hall A dual spectrometer parameters:

$$\Delta\Omega = 7.8 \text{ msr}$$

$$\Delta p/p = \pm 5\%$$

$$L = 1 \cdot 10^{37} \text{ cm}^{-2} \text{ s}^{-1}.$$

The value of L is limited by the estimated singles total counting rates to be less than about $2 \cdot 10^5$ counts/sec (see Table 3), which is about a factor of five less than the expected maximum singles counting rate of 10^6 counts/s.

The coincident counting rates and the true to accidental background ratio (of identified particles) are found to be quite acceptable (see Table 2).

For each pion angle and momentum setting, the coincidence data will be further subdivided into p_m and E_m bins. To reach a total of at least 200 K counts at each spectrometer setting, we will need roughly 1 hour of beam time for high ϵ kinematics, and about 5 hours of beam time for low ϵ kinematics (see Table 2 for counting rate estimates). Thus, a total beam time of about 100 hours ($1 \times 16 + 5 \times 16$) for the ^{12}C target is needed. The running time for other targets is expected to be comparable. We, therefore, request a total of 800 hours of beam time for this proposal to take data for 8 nuclear targets as listed in Sec. IV.

VI. POSSIBLE RELATED MEASUREMENTS

The experimental setup can also be used for other deeply inelastic scattering measurements such as $(e, e' p)$ and $(e, e' K)$ that test different aspects of high energy, low four-momentum transfer nuclear reactions.

VII. CONCLUSION

The proposed measurement of the deeply-inelastic quasifree $(e, e' \pi^{\pm})$ reaction is a good candidate for early scheduling in Hall A. It does not require high resolution on the missing mass spectra; it has relatively large coincident counting rates; and, because this kind of experiment has never been performed on nuclei, it carries the potential for surprise.

Table 1

Number of constituent pions per nucleon
versus atomic weight from Ref. 1

A	N_{π}
2	0.024
4	0.09
27	0.11
56	0.12
208	0.14

Table 2

Counting Rate Estimates for $^{12}\text{C}(\text{e}, \text{e}'\pi^+)$ with Hall A Spectrometers

$$Q^2 = 0.55 \text{ (GeV/c)}^2, \quad q = 2.13 \text{ GeV/c}$$

$$\nu = 2.00 \text{ GeV}, \quad W = 2.02 \text{ GeV}$$

	high $\epsilon = 0.78$ $E_e = 4 \text{ GeV}$ $\theta_e = 15.1^\circ, \theta_q = 14.1^\circ$	low $\epsilon = 0.52$ $E_e = 2.9 \text{ GeV}$ $\theta_e = 26.5^\circ, \theta_q = 10.9^\circ$ [4]
$d\sigma(\text{e}, \text{e}'\pi)$ ($\mu\text{b}/\text{GeV}\text{-sr}^2$)	1.27 ^[1]	0.212 ^[1]
$d\sigma(\text{e}, \text{e}')$ ($\mu\text{b}/\text{GeV}\text{-sr}$)	2.56	0.71
$d\sigma(\text{e}, \pi^+)$ ($\mu\text{b}/\text{GeV}\text{-sr}$)	7.33	5.63
$N_e \text{ (s}^{-1}\text{)} [2]$	$3.994 \cdot 10^4$	$5.001 \cdot 10^3$
$N_\pi \text{ (s}^{-1}\text{)} [2]$	$1.138 \cdot 10^5$	$8.739 \cdot 10^4$
$N_c \text{ (s}^{-1}\text{)} [2]$	$1.55 \cdot 10^2$	$1.16 \cdot 10^1$
$t/a [3]$	$1.71 \cdot 10^1$	$1.33 \cdot 10^1$

[1] Z times proton $d\sigma$ (an underestimate)[2] $\Delta\Omega = 7.8 \text{ msr}$, $\Delta p/p = \pm 5\%$, $L = 1 \cdot 10^{37} \text{ cm}^{-2} \text{ s}^{-1}$

[3] 2 ns resolving time

[4] This angle will be covered by the finite acceptance of the hadron spectrometer positioned at $\theta_{\text{min}} = 12.5^\circ$.

Table 3

Single-Arm Signal and Background Counting Rates on Carbon

		high $\epsilon = 0.78$ $E_e = 4 \text{ GeV}$			low $\epsilon = 0.52$ $E_e = 2.9 \text{ GeV}$		
		$\theta_e = 15.1^\circ$ $p \approx 2 \text{ GeV}/c$	$\theta_q = 14.1^\circ$ $p \approx 2 \text{ GeV}/c$		$\theta_e = 26.5^\circ$ $p \approx 0.9 \text{ GeV}/c$	$\theta_q = 10.9^\circ$ $p \approx 2 \text{ GeV}/c$	
Signal	Particle	e^-	π^+	π^-	e^-	π^+	π^-
	$d\sigma$ ($\mu\text{b}/\text{GeV}\cdot\text{sr}$)	2.56	7.33	7.33	0.71	5.63	5.63
[1] Bkgd	Particle	π^-	p	e^-	π^-	p	e^-
	$d\sigma$ ($\mu\text{b}/\text{GeV}\cdot\text{sr}$)	5.74	7.05	3.20	25.3	6.12	31.5
$\frac{\text{Signal}}{\text{Background}}$		0.45	1.04	2.32	0.028	0.92	0.18
N(total) [2] (10^5 counts/s)		1.295	2.321	1.700	1.832	1.824	5.764

[1] Major background only

[2] $\Delta\Omega = 7.8 \text{ msr}$, $\Delta p/p = \pm 5\%$, $L = 1 \cdot 10^{37} \text{ cm}^{-2} \text{ s}^{-1}$.

REFERENCES

1. B. L. Friman, V. R. Pandharipande, and R. B. Wiringa, Phys. Rev. Lett., **51**, 763 (1983).
2. H. Jung and G. Miller, Pion-Nucleus Physics: Future Direction and New Facilities at LAMPF, 1987, Eds: R. J. Peterson and D. D. Strottman, AIP Conference Proceedings 163.
3. E. L. Berger and F. Coester, Phys. Rev. **D32**, 1071 (1985).
4. J. J. Aubert *et al.*, Phys. Lett. **123B**, 275 (1983).
5. K. Stricker, J. Carr, and H. McManus, Phys. Rev. C **19**, 929 (1979); C **22**, 2043 (1980).
6. J. W. Lightbody, Jr. and J. S. O'Connell, Computers in Physics, May/June, **57** (1988).
7. C. Driver *et al.*, Nucl. Phys. **B32**, 245 (1971).

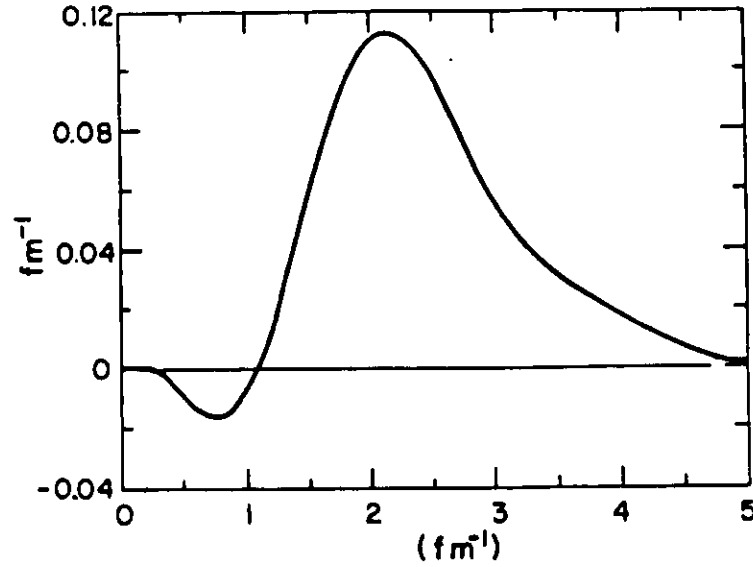


FIG. 1. The function $4\pi p^2 \int \rho_\pi(p, E) dE$ versus p from Ref. 1. This plot shows the momentum spectrum of constituent pions for a nucleus with a Fermi momentum of 1.33 fm^{-1} .

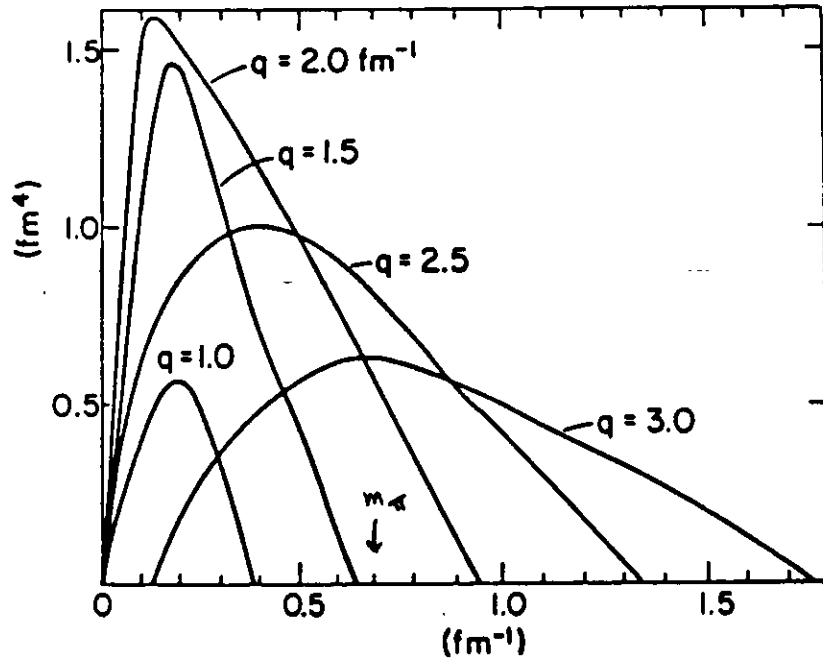


FIG. 2. The function $4\pi p^2 \rho_\pi(p, E)$ versus E from Ref. 2. This plot shows the energy spectrum of the constituent pions for various values of the pion momentum (here called q) in the nuclear ground state, $N_\pi = 0.13$.

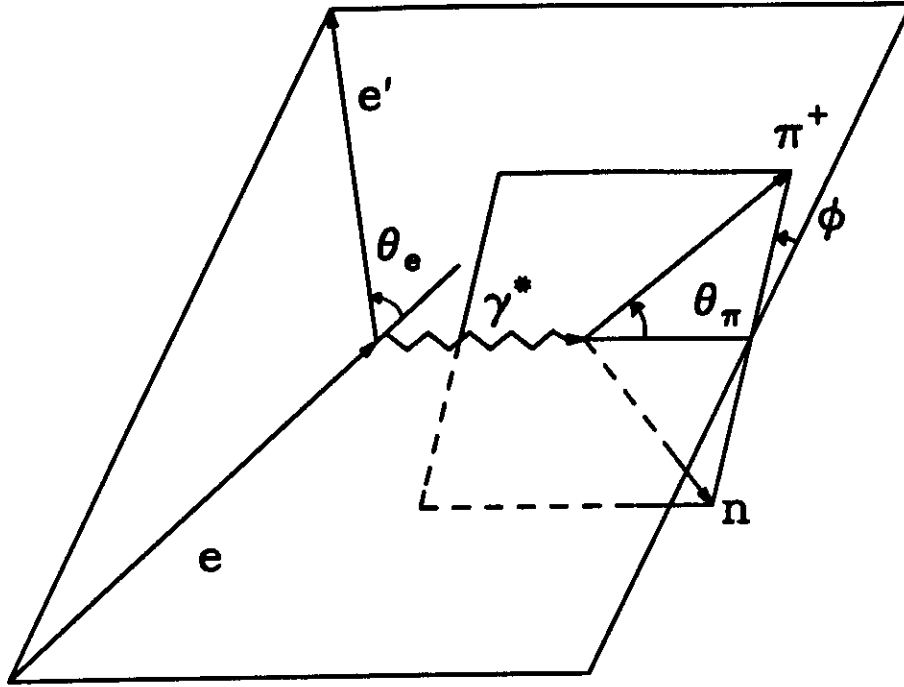


FIG. 3. Kinematics of the electroproduction of pions for the reaction $p(e, e' \pi) n$ in the laboratory system.

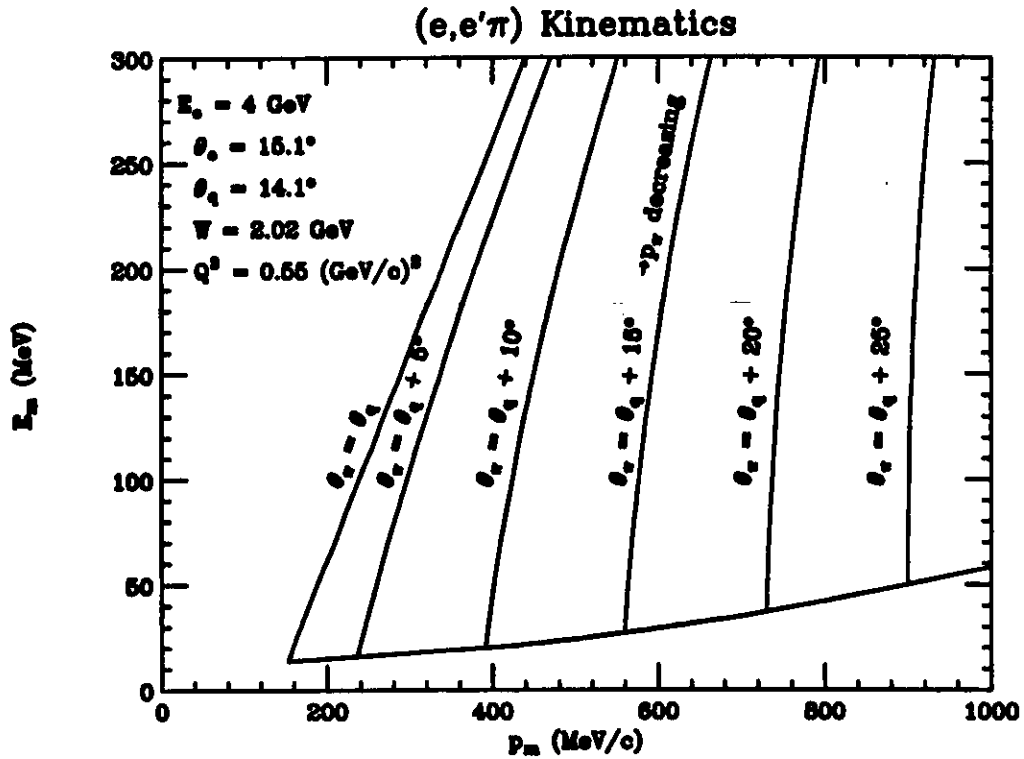


FIG. 4. E_m versus p_m for the kinematic variables indicated.